Chemosphere 89 (2012) 1189–1194

Contents lists available at SciVerse ScienceDirect

Chemosphere

journal homepage: www.elsevier.com/locate/chemosphere

Photoinduced reduction of divalent mercury by quinones in the presence of formic acid under anaerobic conditions

Andrea M. Berkovic [a,b], Sonia G. Bertolotti [c], Laura S. Villata [a], Mónica C. Gonzalez [a], Reinaldo Pis Diez [b], Daniel O. Mártire [a,*]

[a] Instituto de Investigaciones Fisicoquímicas Teóricas y Aplicadas (INIFTA), Facultad de Ciencias Exactas, Universidad Nacional de La Plata, CC 16, Suc. 4, 1900 La Plata, Argentina
[b] Centro de Química Inorgánica (CEQUINOR, CONICET/UNLP), Facultad de Ciencias Exactas, Universidad Nacional de la Plata, CC 962, B1900 AVV La Plata, Argentina
[c] Departamento de Química, Universidad Nacional de Río Cuarto, 5800 Río Cuarto, Argentina

HIGHLIGHTS

- We investigate the mechanism of Hg(II) photo-reduction mediated by naphthoquinone.
- We show that mercury can be eliminated from the solutions as Hg_2Cl_2.
- A commercial fulvic acid can also promote the photo-reduction of Hg(II).

GRAPHICAL ABSTRACT

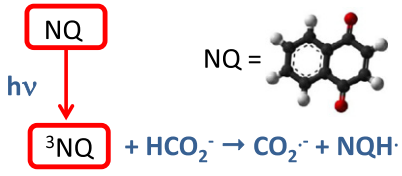

ARTICLE INFO

Article history:
Received 27 April 2012
Received in revised form 11 July 2012
Accepted 12 July 2012
Available online 9 August 2012

Keywords:
Mercury
Mercury photo-reduction
Naphthoquinone
Fulvic acid
DOM triplet states
Flash-photolysis

ABSTRACT

The laser flash photolysis technique (λ^{exc} = 355 nm) was used to investigate the mechanism of the $HgCl_2$ reduction mediated by $CO_2^{\cdot-}$ radicals generated from quenching of the triplet states of 1,4-naphthoquinone (NQ) by formic acid. Kinetic simulations of the experimental signals support the proposed reaction mechanism. This system is of potential interest in the development of UV-A photoinduced photolytic procedures for the treatment of Hg(II) contaminated waters.

The successful replacement of NQ with a commercial fulvic acid, as a model compound of dissolved organic matter, showed that the method is applicable to organic matter-containing waters without the addition of quinones.

1. Introduction

Some metals such as lead, cadmium and mercury are well known for their adverse effects on human health at high levels of exposure. Mercury is released to the atmosphere mainly from fossil fuel combustion, from the degassing of the Earth's crust through volcanoes, and by evaporation from the oceans. In the atmosphere, mercury is transported and transformed into a variety of species with different properties (Lin and Pehkonen, 1999).

Coastal hypoxia events are widespread and increasingly common phenomena, often resulting in seasonal or persistent "dead zones" (Diaz and Rosenberg, 2008). Hypoxic/anoxic conditions at the sediment–water interface have been frequently observed as a consequence of high loadings of organic matter and strong late summer water stratification (Faganeli et al., 2003). In anoxic environments, both bacterial methylation and dissolved organic matter (DOM) reduction occur (Bouffard and Amyot, 2009). In particular, it has been reported that DOM plays a dual role in Hg reduction and release, as DOM is capable of converting Hg(II) to Hg(0), but

* Corresponding author. Tel.: +54 221 4257430; fax: +54 221 4254642.
E-mail addresses: a_berkovic@yahoo.com (A.M. Berkovic), sbertolotti@exa.unrc.edu.ar (S.G. Bertolotti), gonzalez@inifta.unlp.edu.ar (M.C. Gonzalez), pis_diez@quimica.unlp.edu.ar (R. Pis Diez), dmartire@inifta.unlp.edu.ar (D.O. Mártire).

0045-6535/$ - see front matter © 2012 Elsevier Ltd. All rights reserved.
http://dx.doi.org/10.1016/j.chemosphere.2012.07.019

also of reacting with Hg(0) to form Hg-DOM complexes via ligand-induced oxidative complexation (Gu et al., 2011). In fact, low DOM: Hg(II) ratios were suggested to facilitate the reduction of Hg(II) under anoxic conditions.

Aqueous phase Hg(0) formed from the chemical reduction of Hg(II) can be released through the water column to the atmosphere, thereby decreasing Hg availability for microbial methylation. Such process may affect the pool of elemental mercury in aqueous atmospheric and terrestrial compartments and the physical processes regulating its flux to the gaseous phase (Gårdfeldt and Jonson, 2003). Among the photochemical processes for Hg(II) reduction, DOM is well known to significantly enhance the photo-reduction of Hg(II) (Zhang, 2006). Oxalic acid, benzophenone, and humic acid were also shown to affect light-driven reductions of Hg(II) in ice (Bartels-Rausch et al., 2011).

Conventional technologies for treating wastewater containing heavy metals include coagulation (Akbal and Camci, 2010), chemical precipitation (Lewis, 2010), ion exchange (Smara et al., 2007), membrane separation (Gabor and Endre, 2009) and adsorption (Zhou and Haynes, 2010). After the application of one treatment method or a combination of several methods, a sludge containing heavy metals is obtained.

With the aim of obtaining the basic knowledge necessary for developing a method for treating heavy metals-containing waters, which enables mercury separation prior the application of conventional technologies, previous investigations of our group were devoted to elucidate the mechanism of the reduction of $HgCl_2$ to Hg_2Cl_2 mediated by the $CO_2^{\cdot-}$ radicals (Berkovic et al., 2010). The $CO_2^{\cdot-}$ radicals were generated by UV-C ($200 \leqslant \lambda \leqslant 290$ nm) photolysis of $S_2O_8^{2-}$ solutions in the presence of formate ions or formic acid (Rosso et al., 2001; Berkovic et al., 2010). From an environmental point of view, the use of activated peroxydisulfate in the presence of formate as an additive is a convenient method for the mineralization of some substrates (Mora et al., 2009) since it has the advantage that leaves no toxic residues. However, the development of a photochemical method which employs sunlight instead of UV-C sources is more attractive.

Among the additives that absorb in the visible range and are capable of producing $CO_2^{\cdot-}$ radicals are quinones. In particular, 1,4-naphthoquinone (NQ) absorbs in the UV-A region of the electromagnetic spectrum ($320 \leqslant \lambda \leqslant 400$ nm) within the solar radiation reaching the Earth's surface, and the reduction of its lowest triplet state (^{3}NQ) by formate ions generates the reducing $CO_2^{\cdot-}$ radicals (reaction (1) in Table 1) (Loeff et al., 1991; Görner, 2007). Quinones are found in the environment as products of fuel combustion, tobacco smoke, plants, and in fulvic substances, one of the major components of DOM in natural waters (Kumagai et al., 2012). Exposure of cultured cells and experimental animals to NQs promotes not only inflammation but also anti-inflammation; most of the studied exhibit anticancer effects. Therefore, we thus set out to investigate the complex reaction mechanism involved in the one-electron reduction of $HgCl_2$ mediated by $CO_2^{\cdot-}$ radicals generated by laser flash-photolysis (LFP) of NQ (λ^{exc} = 355 nm). This system is of potential interest in the development of UV-A photoinduced photolytic procedures for the treatment of Hg(II) contaminated waters and to further understand Hg(II) reduction in the environment. Because quinones are present in fulvic substances, the reduction of $HgCl_2$ photopromoted by a commercial fulvic acid in the presence of formic acid was also investigated.

2. Material and methods

2.1. Materials

NaHCOO, HCOOH, and $HClO_4$, $HgCl_2$ from J.T. Baker; methyl viologen dichloride [$MVCl_2$], and NQ from Sigma–Aldrich were used without further purification. Pahokee Peat fulvic acid was from the International Humic Substance Society. Deionized water (>18 MΩ cm, <20 ppb of organic carbon) was obtained from a Millipore system.

All mercury working solutions were freshly prepared prior to each experiment. The temperature of the solutions was 298 K controlled to ±1 K with a Grant model GD 1200 thermostat.

The pH of the $HgCl_2$ solutions was set in the range 1–2 because of the low solubility of this salt at higher pH (Powell et al., 2005).

2.2. Methods

2.2.1. LFP experiments

LFP experiments were performed by excitation with the third harmonic (355 nm) of a Nd:YAG Spectron SL 400 laser (18 ns FWHM). The instrumentation has been described elsewhere

Table 1
Reaction mechanism.

	Reactions	Rate constant	$\Delta_{ET}G^\circ$ (kJ mol^{-1})
(R1)	$^3NQ + HCOOH \rightarrow H^+ + CO_2^{\cdot-} + NQH^\cdot$	3×10^9 M^{-1} s^{-1}[a]	−124
(R2)	$MV^{2+} + CO_2^{\cdot-} \rightarrow CO_2 + MV^{\cdot+}$	6.3×10^9 M^{-1} s^{-1}[b]	−145
(R3)	$MV^{\cdot+} + MV^{\cdot+} \rightarrow (MV)_2^{2+}$	1.5×10^{10} M^{-1} s^{-1}[c]	–
(R4)	$NQH^\cdot + MV^+ \rightarrow MV^{2+} + NQ^{2-} + H^+$	$(4.5 \pm 0.5) \times 10^{10}$ M^{-1} s^{-1}[d]	−130
(R5)	$^3NQ + H^+ + CO_2^{\cdot-} \rightarrow CO_2 + NQH^\cdot$	4×10^9 M^{-1} s^{-1}[a]	−444
(R6)	$NQH^\cdot + NQH^\cdot \rightarrow NQ^{2-} + NQ + 2H^+$	7.3×10^8 M^{-1} s^{-1}[d]	−13
(R7)	$^3NQ + Cl^- + H^+ \rightarrow NQH^\cdot + Cl^\cdot$	1.7×10^9 M^{-1} s^{-1}[a]	−5
(R8)	$NQ + MV^{\cdot+} + H^+ \rightarrow MV^{2+} + NQH^\cdot$	$(4.0 \pm 0.8) \times 10^9$ M^{-1} s^{-1}[d]	−60
(R9)	$^3NQ + MV^{\cdot+} + H^+ \rightarrow MV^{2+} + NQH^\cdot$	$(1.0 \pm 0.2) \times 10^9$ M^{-1} s^{-1}[d]	−30
(R10)	$NQ + CO_2^{\cdot-} + H^+ \rightarrow CO_2 + NQH^\cdot$	4×10^9 M^{-1} s^{-1}[a]	−20
(R11)	$^3NQ + H_2O \rightarrow P$	5.5×10^6 s^{-1}[d]	–
(R12)	$NQH^\cdot + H_2O \rightarrow P'$	1.7×10^4 s^{-1}[d]	–
(R13)	$CO_2^{\cdot-} + HgCl_2 \rightarrow CO_2 + HgCl + Cl^-$	1.8×10^8 M^{-1} s^{-1}[c]	−148
(R14)	$HgCl_2 + MV^{\cdot+} \rightarrow MV^{2+} + HgCl + Cl^-$	6×10^7 M^{-1} s^{-1}[c]	2
(R15)	$NQ + HgCl + H^+ + Cl^- \rightarrow HgCl_2 + NQH^\cdot$	–	−57
(R16)	$^3NQ + HgCl + H^+ + Cl^- \rightarrow HgCl_2 + NQH^\cdot$	–	−296

[a] From (Loeff et al., 1991).
[b] From (Das et al., 2003).
[c] From (Berkovic et al., 2010).
[d] From this work.

(Bertolotti and Previtali, 1997). The detection comprises a PTI monochromator coupled to a photomultiplier tube R666 Hamamatsu attached to a digital oscilloscope (HP54504). The laser beam was defocused to cover the full optical path of the beam scanner (10 mm) from a 150 W xenon lamp.

Due to the high absorbance of the solutions below 300 nm, the direct detection of $CO_2^{\cdot-}$ and of Hg(I) (Berkovic et al., 2010) was not possible. Thus, since the $CO_2^{\cdot-}$ radicals are able to reduce methyl viologen (MV^{2+}) to the $MV^{\cdot+}$ radical (λ^{max} = 393 nm) (Das et al., 2003), MV^{2+} was employed as a probe.

2.2.2. Determination of total mercury

Ar-saturated aqueous solutions containing 0.25 mM of NQ, 0.4 M of HCOOH, and 3.8 mM $HgCl_2$ (pH = 2) were irradiated with the third harmonic (λ = 355 nm) of a Continuum Nd:YAG laser (15 mJ/pulse at a repetition rate of 10 Hz) in 1 × 1 cm quartz fluorescence cuvettes.

The photolysis times were shorter than 2 h. The irradiated solutions were centrifuged at 7000 rpm for 20 min. Total mercury was quantified in the supernatant by cold vapor atomic absorption (EPA SW 846 M 7470 EAA Cold Vapor) with a Varian Spectraa-55 equipment.

2.2.3. Raman spectra

In order to collect an appreciable amount of the precipitate to be analyzed by Raman spectroscopy, 250 mL of an Ar-saturated 0.25 mM solution of NQ containing 0.4 M HCOOH, and 3.8 mM $HgCl_2$ at pH = 2 were irradiated for 5 h with six 350 nm lamps from a RPR-100 Rayonet. Raman spectra of the solid were recorded using a LabRAM HR Raman system (Horiba Jobin Yvon), equipped with a confocal microscope, two monochromator gratings and a charge coupled device detector. An 1800 g mm^{-1} grating and 100 mm hole results in a 2 cm^{-1} spectral resolution. The 514.5 nm line of an Ar^+ laser was used as excitation source. Measurements were carried out in a backscattering geometry, with an objective magnification of 10×. Acquisition time was 60 s and 10 accumulations.

2.2.4. Computer simulations

A computer program based on component balances formulated in terms of a Differential Algebraic Equations system, which is solved by the Runge Kutta method was used to simulate the LFP signals (David Gara et al., 2008). The program considers the pulsed excitation as a delta function, producing the ^{3}NQ. The concentration of ^{3}NQ present immediately after excitation was taken as an input parameter, estimated from the experiments performed the absence of HCOOH, $MVCl_2$ and $HgCl_2$.

3. Results and discussion

3.1. Detection of ^{3}NQ

LFP experiments (λ^{exc} = 355 nm) performed with an Ar-saturated aqueous solution (pH = 2) containing 0.25 mM NQ showed formation of a transient species characterized by a single exponential decay with lifetime τ = (0.13 ± 0.01) μs. The absorption spectra taken at different times after the laser shot are shown in Fig. 1. The relatively good agreement of this spectrum measured at pH = 2 with that previously obtained with neutral solutions (Loeff et al., 1991) supports the assignment of the transient species to lowest triplet state of NQ.

3.2. Reaction of ^{3}NQ with formic acid

The inset of Fig. 2 shows the signals obtained at 360 and 430 nm. As previously reported (Loeff et al., 1991), the $HCOO^-$ ion is able to transfer an electron to ^{3}NQ at pH = 8 solutions. The corresponding electron transfer process under our pH conditions is shown in reaction (1) of Table 1. Note that the conjugate acid $NQH^{\cdot}$ radical (pKa = 4.1) (Patel and Willson, 1973) is included as product of reaction (1) instead of the radical anion. Assuming for the rate constant k_1 the value reported for the electron transfer at pH = 8 (3×10^9 M^{-1} s^{-1}, Table 1), and considering the concentration of HCOOH used in the experiments (0.4 M), the expected ^{3}NQ lifetime in our conditions is <1 ns. Thus, the transient species observed in the conditions shown in Fig. 2 is assigned to the $NQH^{\cdot}$ radical, because the other product ($CO_2^{\cdot-}$) does not absorb in the wavelength range of measurement. The good agreement between the absorption spectrum of $NQH^{\cdot}$ obtained here and that reported previously (Patel and Willson, 1973) is shown in Fig. 1.

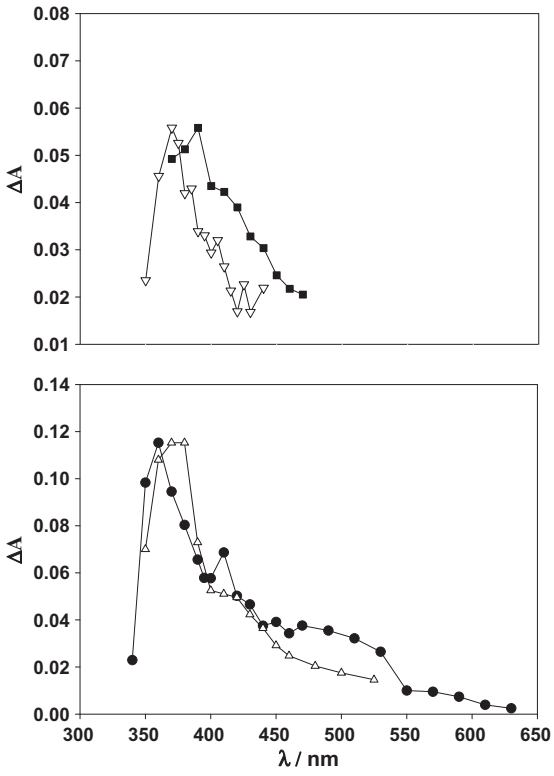

Fig. 1. Top: absorption spectrum of ^{3}NQ obtained at t = 0 with Ar-saturated 0.25 mM solutions of NQ at pH = 2 (▽). The normalized reported spectrum of ^{3}NQ at pH = 7 (■) is also shown. Bottom: absorption spectrum of $NQH^{\cdot}$ obtained at t = 0 with Ar-saturated 0.25 mM solutions of NQ containing 0.4 M of HCOOH at pH = 2 (●). The normalized reported spectrum of NQH (?) obtained at pH = 2 is also shown (Patel and Willson, 1973).

The absorption spectrum obtained at t = 0 after the laser shot (λ^{exc} = 355 nm) with an Ar-saturated aqueous solution (pH = 2) containing 0.25 mM NQ and 0.4 M HCOOH is shown in Fig. 1. Comparison of this spectrum to that previously obtained for the $NQH^{\cdot}$ radical (Patel and Willson, 1973) further supports the assignment.

The decay of the $NQH^{\cdot}$ radical followed a mixed first and second order kinetics according to Eq. (1):

$$\Delta A = \frac{k_{first}}{b \times \exp(k_{first} \times t) - c} \quad (1)$$

$\Delta A(t)$ is the time-dependent absorbance, $c = 2k_6/(\varepsilon l)$ with ε the absorption coefficient and l = 1 cm, the optical pathlength; $b = c + k_{first}/\Delta A_0$ with k_{first}: the pseudo first order decay rate constant, k_6: the rate constant of reaction (6) in Table 1 and ΔA_0: the value of ΔA(t) extrapolated to t = 0. From fitting of the data to Eq. (1) the values of k_6 and $k_{first} = k_{12}$ (see Table 1) are obtained.

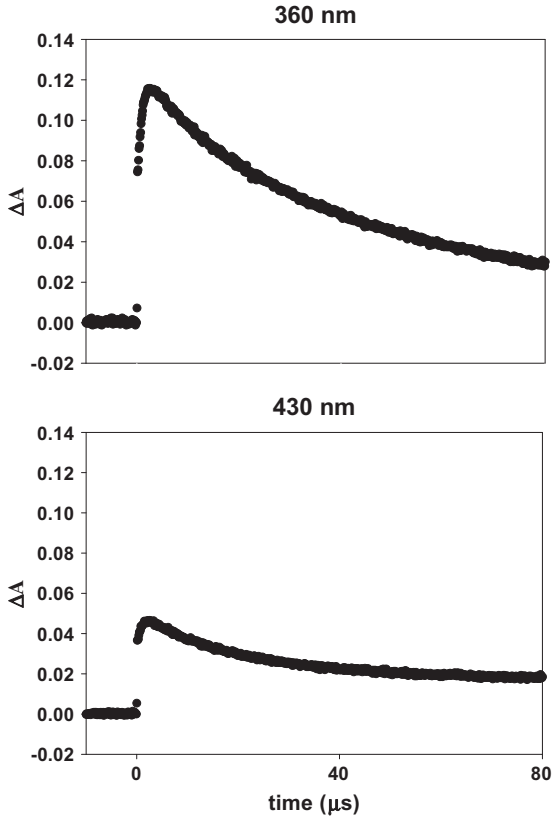

Fig. 2. Absorbance changes at 360 and 430 nm obtained from LFP experiments (λ^{exc} = 355 nm) performed with an Ar-saturated aqueous solution (pH = 2) containing 0.25 mM NQ and 0.4 M HCOOH.

3.3. Reaction of $CO_2^{\cdot-}$ with MV^{2+}

MV^{2+} was employed as a competitive scavenger of the $CO_2^{\cdot-}$ radicals in the solutions containing $HgCl_2$ (see below) (Berkovic et al., 2010). LFP experiments with Ar-saturated aqueous solutions (pH = 2) containing 0.25 mM NQ, 0.4 M HCOOH, and 0.1 mM $MVCl_2$ were performed. Under these conditions reaction (2) in Table 1 takes place. Thus, the signal obtained at 390 nm, the absorption maximum of $MV^{\cdot+}$ ($\varepsilon = 4.21 \times 10^4\ M^{-1}\ cm^{-1}$) (Watanabe and Honda, 1982), is expected to contain contributions of both $MV^{\cdot+}$ and $NQH^{\cdot}$. The signal obtained at this wavelength (Fig. 3) shows two decay components: a faster decay and a slower one. The rate of the latter is similar to that measured for the $NQH^{\cdot}$ radical in the absence of MV^{2+}, and thus is assigned to this species; whereas the faster decay should be due to $MV^{\cdot+}$. This is confirmed below by the kinetic simulation of the signals.

The experiments could be reproduced by the simulation taking 8.0×10^{-6} M for the initial concentration of ^3NQ. This value was estimated from the absorption at $t = 0$ measured in the LFP experiments performed in the absence of HCOOH and $MVCl_2$, and taking $\varepsilon^{390} = 3000\ M^{-1}\ cm^{-1}$ for the absorption coefficient of ^3NQ (Loeff et al., 1991).

The mechanism employed for the simulations (reactions (1)–(12) in Table 1) includes some well reported reactions, as those involving reactions (1), (5), (7) and (10) (Loeff et al., 1991), reaction (2) (Das et al., 2003), and reaction (3) (Berkovic et al., 2010). Also included are reactions (6), (11) and (12). The rate constant k_{11} was set equal to the reciprocal of the triplet lifetime in the absence of formate (see above). The rate constants of reactions (6) and (12) were obtained from a mixed first and second order rate law of the signal measured in the absence of $MVCl_2$ (see above).

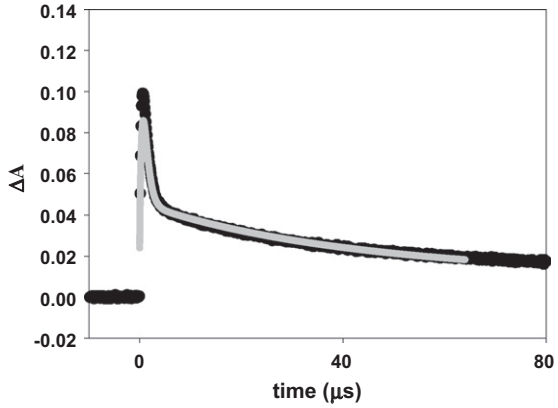

Fig. 3. Absorbance change obtained at 390 nm with an Ar-saturated aqueous solution (pH = 2) containing 0.25 mM NQ, 0.4 M HCOOH, and 0.10 mM $MVCl_2$. The grey line shows the computer simulation.

To prove the complex reaction mechanism, computer simulations were performed. However, this simple reaction set cannot account for the observed signals, and reactions (4), (8) and (9), were also considered. The calculated negative change of standard Gibbs energy, $\Delta_{ET}G^{\circ}$, indicate that these reactions are thermodynamically feasible. The values of $\Delta_{ET}G^{\circ}$ listed in Table 1 were calculated as recommended elsewhere (Braslavsky, 2007). The details are given in the Supplementary Material.

The rate constants of reactions (4), (8) and (9) were systematically varied until the best coincidence (best residuals distribution) between experimental and simulated signals taken at 390 nm was obtained. The simulated signal at 390 nm was obtained from the molar absorption coefficients (in parentheses) and concentration profiles of the following species: ^3NQ ($3000\ M^{-1}\ cm^{-1}$), $NQH^{\cdot}$ ($3200\ M^{-1}\ cm^{-1}$), $MV^{\cdot+}$ ($42100\ M^{-1}\ cm^{-1}$) (Watanabe and Honda, 1982), and NQ^{2-} ($2000\ M^{-1}\ cm^{-1}$). The molar absorption coefficients of ^3NQ, $NQH^{\cdot}$, and NQ^{2-} were comparable to those reported in (Loeff et al., 1991) and (Patel and Willson, 1973).

The good agreement between experimental and simulated signals (Fig. 3) supports the proposed mechanism.

3.4. Photoinduced reduction of $HgCl_2$

Under the experimental conditions employed in the LFP experiments (0.2 mM < total $[Cl^-]$ < 10.2 mM), the aqueous soluble $HgCl_2$ complex is the main Hg(II) species in solution (Stability constant = $10^{13.2}$) (Powell et al., 2005). Formation of Hg(II)-formate complexes is negligible, since, the Hg(II) complexes with chloride ions present much higher stability constants than those of carboxylic acids (Lin and Ariya, 2008). The one-electron reduction of $HgCl_2$ yields HgCl and chloride anions, and further dimerization of HgCl leads to Hg_2Cl_2 (Berkovic et al., 2010), the following reaction:

$$2HgCl \rightarrow Hg_2Cl_2 \qquad (R17)$$

The extremely low solubility of the latter product (Ksp = 5×10^{-20}) (Pokrovskiy, 1996) ensures its removal from solution, and therefore, it is not involved in further redox reactions.

The formation of Hg_2Cl_2(s) was confirmed by Raman spectroscopy of the solid. The spectrum (see Fig. 4) shows the bands at 167.8 and 275.2 cm^{-1} assigned to the ClHg–HgCl ($\nu_2\sum_g^+$) and Hg–Cl ($\nu_1\sum_g^+$) stretching modes, respectively (Brolo et al., 2002).

The complete reaction mechanism for the system containing $HgCl_2$ considers reactions (1)–(15) in Table 1. Reaction (16) was not considered because the simulations show that when HgCl is formed the concentration of ^3NQ is already negligible.

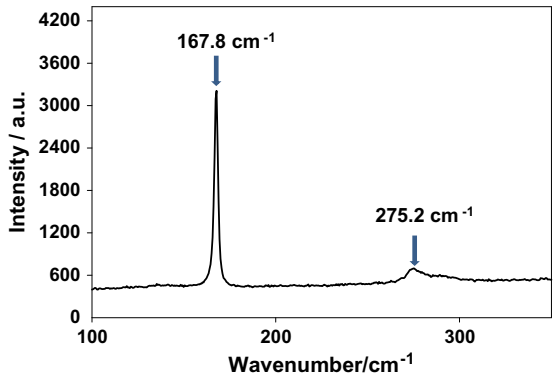

Fig. 4. Raman spectrum of the solid obtained as product of the photochemical reaction. The bands assigned to the ClHg–HgCl and Hg–Cl stretching modes (see Brolo et al., 2002) are shown.

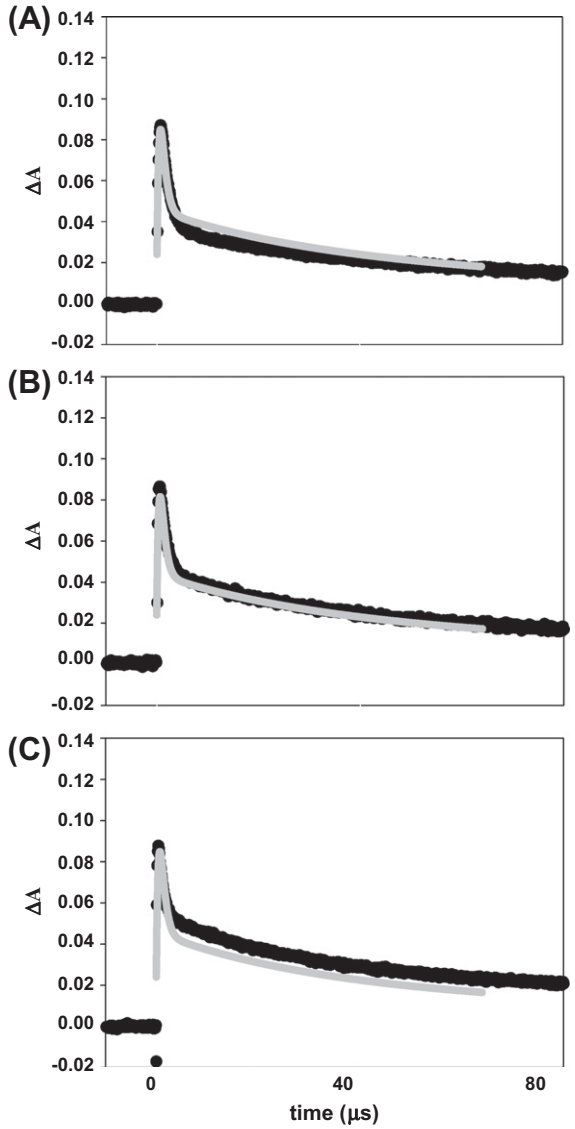

Fig. 5. Absorbance changes obtained at 390 nm with an Ar-saturated aqueous solution (pH = 2) containing 0.25 mM NQ, 0.4 M HCOOH, 0.10 mM $MVCl_2$, and different amounts of $HgCl_2$: (A) 0.2 mM, (B) 0.5 mM, and (C) 1 mM. The grey lines show the computer simulations.

For the simulations of the experimental signals the rate constants of reactions (13) and (14) were taken from our previous paper (Berkovic et al., 2010). The inclusion of reaction (15) with a rate constant of $1 \times 10^{10}\ M^{-1}\ s^{-1}$ did not affect the simulations. Therefore reaction (15) is of little significance under our experimental conditions.

The comparison of experimental and simulated signals at 390 nm for three solutions containing different amounts of $HgCl_2$ is shown in Fig. 5. Given the complexity of the system, the agreement between simulated and experimental signals is good.

3.5. Evolution of the concentration of total dissolved mercury

Upon irradiation at 355 nm of an Ar-saturated aqueous solution (pH = 2) containing 0.25 mM NQ, 0.4 M formic acid, and 3.8 mM $HgCl_2$ the appearance of a solid is observed, in agreement with reaction (17).

The evolution of the concentration of total dissolved mercury is shown in Fig. 6.

As can be seen in Fig. 6 (top), after 90 min of irradiation of the 3.8 mM $HgCl_2$ solution, the concentration of total mercury decreases to about 80% of the initial value. This result shows the high efficiency of the method.

Because quinones are present in humic substances, the major component of DOM in natural waters, the generation of the reducing $CO_2^{\bullet-}$ radicals in DOM-containing waters could be achieved without the addition of NQ. To prove this hypothesis Ar-saturated solutions containing Pahokee Peat fulvic acid, HCOOH and $HgCl_2$ were irradiated at 355 nm. Precipitation of Hg_2Cl_2 upon irradiation was observed and the decrease of the total concentration of mercury is shown in Fig. 6 (bottom). As can be seen in Fig. 6, there is a slight

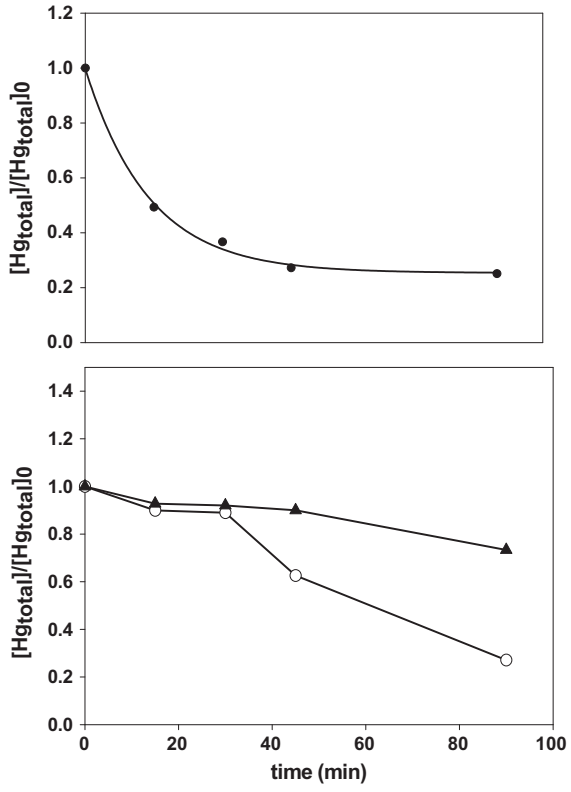

Fig. 6. Relative decay of the total concentration of mercury obtained upon irradiation at 355 nm of Ar-saturated aqueous pH = 2 solutions containing: Top: 0.25 mM NQ, 0.4 M HCOOH, and 3.8 mM $HgCl_2$. The line shows the fitting of the data to an exponential decay function. Bottom: 50 ppm pahokee peat fulvic acid and 0.15 mM Hg(II) without (▲) and with (○) 0.4 M HCOOH.

depletion of the total mercury concentration upon irradiation of the solution without HCOOH (black triangles), which is in agreement with the reported photoreduction of Hg^{2+} by humic substances (Xiao et al., 1995). However, the decrease of the total mercury concentration is significantly enhanced in the presence of HCOOH (white circles), which is in line with $CO_2^{\bullet-}$ mediated pathways.

4. Conclusions

The mechanism of the photoreduction of $HgCl_2$ promoted by NQ in the presence of formic acid was investigated by means of LFP and computer simulation of the experimental signals.

It was shown here that anaerobic UV-A irradiation of NQ solutions containing formic acid results in the photo-reduction of $HgCl_2$ followed by precipitation of Hg_2Cl_2, which can be easily removed by filtration. These results are of potential interest for the development of technical systems for the treatment of waters contaminated with $HgCl_2$.

The successful replacement of NQ with a commercial fulvic acid, as a model compound of dissolved organic matter, showed that the method could be applied to organic matter-containing waters without the addition of quinones.

The knowledge of the kinetic information of some of the elementary steps of the reaction mechanism could also be relevant for modeling reactions taking place under anoxic environmental conditions.

Acknowledgements

This work has been supported by grants PICT 2007#00308 and PICT 2008#00686 from ANPCyT, Argentina. A.M.B. thanks CONICET for a graduate studentship. S.G.B., M.C.G., and R.P.D. are research members of CONICET, Argentina. L.S.V. and D.O.M. are research members of CIC, Buenos Aires, Argentina. The authors thank the group of vibrational spectroscopy from Comisión Nacional de Energía Atómica (CNEA, Argentina) for the Raman spectra.

Appendix A. Supplementary material

Supplementary data associated with this article can be found, in the online version, at http://dx.doi.org/10.1016/j.chemosphere.2012.07.019.

References

Akbal, F., Camci, S., 2010. Comparison of electrocoagulation and chemical coagulation for heavy metal removal. Chem. Eng. Technol. 33, 1655–1664.

Bartels-Rausch, T., Krysztofiak, G., Bernhard, A., Schläppi, M., Schwikowski, M., Ammann, M., 2011. Photoinduced reduction of divalent mercury in ice by organic matter. Chemosphere 82, 199–203.

Berkovic, A.M., Gonzalez, M.C., Russo, N., Michelini, M., Pis Diez, R., Mártire, D.O., 2010. The reduction of Hg(II) by the carbon dioxide radical anion: a theoretical and experimental investigation. J. Phys. Chem. A 114, 12845–12850.

Bertolotti, S.G., Previtali, C.M., 1997. The excited states quenching of safranine T by p-benzoquinones in polar solvents. J. Photochem. Photobio. A 103, 115–119.

Bouffard, A., Amyot, M., 2009. Importance of elemental mercury in lake sediments. Chemosphere 74, 1098–1103.

Braslavsky, S.E., 2007. Glossary of terms used in photochemistry, third ed., Pure Appl. Chem. 79, 293–465.

Brolo, A.G., Odziemkowski, M., Porter, J., Irish, D.E., 2002. In situ microRaman investigation of electrochemically formed halide and pseudohalide films on mercury electrodes. J. Raman Spectrosc. 33, 136–141.

Das, T.N., Ghanty, T.K., Pal, H., 2003. Reactions of methyl viologen dication (MV^{2+}) with H atoms in aqueous solution: mechanism derived from pulse radiolysis measurements and ab initio MO Calculations. J. Phys. Chem. A 107, 5998–6006.

David Gara, P.M., Bosio, G.N., Gonzalez, M.C., Mártire, D.O., 2008. Kinetics of the sulfate radical – mediated photooxidation of humic substances. Int. J. Chem. Kinet. 40, 19–24.

Diaz, R.J., Rosenberg, R., 2008. Spreading dead zones and consequences for marine ecosystems. Science 321, 926–929.

Faganeli, J., Horvat, M., Covelli, S., Fajon, V., Logar, M., Lipej, L., Cermelj, B., 2003. Mercury and methylmercury in the gulf of trieste (northern Adriatic Sea). Sci. Total Environ. 304, 315–326.

Gabor, B., Endre, N., 2009. Removal of zinc and nickel ions by complexation membrane filtration process from industrial wastewater. Desalination 240, 218–226.

Gårdfeldt, K., Jonson, M., 2003. Is bimolecular reduction of Hg(II) complexes possible in aqueous systems of environmental importance. J. Phys. Chem. A107, 4478–4482.

Görner, H., 2007. Oxygen uptake upon photolysis of 1,4-benzoquinones and 1,4-naphthoquinones in air-saturated aqueous solution in the presence of formate, amines, ascorbic acid, and alcohols. J. Phys. Chem. 111, 2814–2819.

Gu, B., Bian, Y., Miller, C.L., Dong, W., Jiang, X., Liang, L., 2011. Mercury reduction and complexation by natural organic matter in anoxic environments. Proc. Natl. Acad. Sci. USA 108, 1479–1483.

Kumagai, Y., Shinkai, Y., Miura, T., Cho, A.K., 2012. The chemical biology of naphthoquinones and its environmental implications. Ann. Rev. Pharmacol. Toxicol. 52, 221–247.

Lewis, A.E., 2010. Review of metal sulphide precipitation. Hydrometallurgy 104, 222–234.

Lin, S., Ariya, P.A., 2008. Reduction of oxidized mercury species by dicarboxylic acids (C2–C4): kinetic and product studies. Environ. Sci. Technol. 42, 5150–5155.

Lin, C.J., Pehkonen, S.O., 1999. The chemistry of atmospheric mercury: a review. Atmos. Environ. 33, 2067–2079.

Loeff, I., Goldstein, S., Treinin, A., Linschitz, H., 1991. Interactions of formate ion with triplets of anthraquinone-2-sulfonate, 1,4-naphthoquinone, benzophenone-4-carboxylate and benzophenone-4-sulfonate. J. Phys. Chem. 95, 4423–4430.

Mora, V.C., Rosso, J.A., Carrillo Le Roux, G., Mártire, D.O., Gonzalez, M.C., 2009. Thermally activated peroxydisulfate in the presence of additives: a clean method for the degradation of pollutants. Chemosphere 75, 1405–1409.

Patel, K.B., Willson, R.L., 1973. Semiquinone free radicals and oxygen. Pulse radiolysis study of one electron transfer equilibria. J. Chem. Soc. Trans. I 69, 814–825.

Pokrovskiy, O.S., 1996. Measurement of the stability constant of an Hg(I) chloride complex in aqueous solutions at 20–80 °C. Geochem. Int. 33, 83–97.

Powell, K.J., Brown, P.L., Byrne, R.H., Gajda, T., Hefter, G., Sjoberg, S., Wanner, H., 2005. Chemical speciation of environmentally significant heavy metals with inorganic ligands part 1: the Hg^{2+}–Cl^-, OH^-, CO_3^{2-}, SO_4^{2-}, and PO_4^{3-} aqueous systems. Pure Appl. Chem. 77, 739–800.

Rosso, J.A., Bertolotti, S.G., Braun, A.M., Mártire, D.O., Gonzalez, M.C., 2001. Reactions of carbon dioxide radical anion with substituted benzenes. J. Phys. Org. Chem. 14, 300–309.

Smara, A., Delimi, R., Chainet, E., Sandeaux, J., 2007. Removal of heavy metals from diluted mixtures by a hybrid ion-exchange/electrodialysis process. Sep. Purif. Technol. 57, 103–110.

Watanabe, T., Honda, K., 1982. Measurement of the extinction coefficient of the methyl viologen cation radical and the efficiency of its formation by semiconductor photocatalysis. J. Phys. Chem. 86, 2617–2619.

Xiao, Z.F., Stromberg, D., Lindqvist, O., 1995. Reduction of mercury(II) by tropical river humic substances (Rio Negro)/Part II. Influence of structural features (molecular size, aromaticity, phenolic groups, organically bound sulfur). Water, Air, Soil Pollut. 80, 789–798.

Zhang, H., 2006. Photochemical redox reactions of mercury. Struct. Bond. 120, 37–79.

Zhou, Y.F., Haynes, R.J., 2010. Sorption of heavy metals by inorganic and organic components of solid wastes: significance to use of wastes as low-cost adsorbents and immobilizing agents. Crit. Rev. Environ. Sci. Technol. 40, 909–977.